DTP-96/60
July, 1996

Chiral poles and zeros and the role of the left hand cut

M. Boglione [1,2]

and

M.R. Pennington [1]

[1] *Centre for Particle Theory, University of Durham Durham DH1 3LE, U.K.*

[2] *Dipartimento di Fisica Teorica, Università di Torino and INFN, Sezione di Torino, Via P. Giuria 1, 10125 Torino, Italy*

Abstract

It has been recently claimed that the Inverse Amplitude Method provides a reliable unitarisation of Chiral Perturbation Theory allowing resonance poles to be accurately uncovered. We illustrate the sensitivity of these claims to the treatment of the Adler zero and to assumptions about the left hand cut (and hence about the underlying exchange forces). Previously favoured methods are shown to mistreat the Adler zeros and violate crossing symmetry casting doubt on the precision of their phenomenology. A more reliable solution is proposed.

1. Introduction

Developments in chiral perturbation theory (χPT) have led to a resurgence of interest in low energy $\pi\pi$ scattering [1, 2]. The predictions of χPT unambiguously apply to the $\pi\pi$ process in the subthreshold region. Chiral dynamics demands that $\pi\pi$ and πK amplitudes have zeros below threshold. These are the on-shell appearance of the Adler zero and they occur in each S-wave amplitude [3]. These zeros of course occur in physical amplitudes.

Recently, much attention has been paid to how to compare the predictions of χPT with experiment [4, 5]. A key discussion point concerns how far one can reliably continue the χPT amplitudes above threshold to where experimental information exists? It is a feature of the physical world that resonances dominate the behaviour of isospin $I \leq 1$ partial waves. Resonances, however, do not appear in χPT at any finite order, since low energy resonant amplitudes are non-perturbative in their fulfillment of unitarity. Consequently, the issue of how to extract resonance physics from the chiral expansion has been a topic of heated debate [4, 5].

Dispersion relations provide an invaluable connection between scattering amplitudes in one energy region and another. They connect the subthreshold region where χPT applies and the world of resonance physics. However, their evaluation requires knowledge not just of the singularity structure of the amplitude, but of the exact form of its discontinuity across any cut; for example we must know the imaginary part to determine the real part of each amplitude. A seemingly significant advantage of considering the dispersive representation of the inverse of a partial wave amplitude is that its right hand cut discontinuity is just given by phase space in the elastic region, thanks to unitarity. Consequently, when the integral along this cut is controlled by the low energy region, it can be evaluated reliably without any further information. While what we might regard as "kinematics" fixes the right hand cut, dynamics is built in by assumptions about the left hand cut. Indeed, this is the basis of the N/D method [6].

While partial wave amplitude, $t(s)$, have right and left hand cuts, unitarity does not allow them to have poles on the physical sheet. As a consequence, their inverses, $f(s)$,

have similar right and left cuts. However, partial wave amplitudes can and do have zeros, which in turn means their inverses have poles on the physical sheets, making their singularity structure a little more complicated. These poles are the essence of chiral dynamics.

Very recently Dobado and Peláez [7] have used dispersion relations for the inverse $\pi\pi$ and πK amplitudes and ignored the appearance of such poles. This has allowed them to *derive* a Padé-like approximant as the sum of chiral perturbative predictions for the S-wave amplitudes, rather like that much used for the P-wave [8]. Their choice of approximations gives a description that does agree with experiment. However, we show here how strongly these essentially dispersive continuations of the predictions of χPT depend on

(i) the left hand cut discontinuity,

(ii) the existence of chiral poles,

(iii) additional summation assumptions implicit in the Padé approximation.

Indeed, within each set of assumptions, good agreement with experiment below 800 MeV is possible, depending on different choices of the $\mathcal{O}(p^4)$ χPT parameters $\overline{\ell}_i$ for $i = 1, 2$ [1]. Thus this is not a reliable way of determining the $\overline{\ell}_i$.

In the next section we give a general introduction to an inverse amplitude method and the treatment of chiral poles. We propose several alternative forms for the left hand cut discontinuity and in sect. 3 show how the physical region results depend on these. In Sect. 4 we give our brief conclusions.

2. The amplitude and its inverse

Consider the $\pi\pi$ partial wave amplitudes, $t^I_J(s)$, with isospin I and spin J. Defining s to be usual square of the c.m. energy and denoting the pion mass by μ, elastic unitarity

requires

$$\text{Im } t_J^I(s) = \rho(s) \mid t_J^I(s) \mid^2 \tag{1}$$

where $\rho(s) \equiv \sqrt{1-4\mu^2/s}$. In practice, the first significant inelastic channel opens up only at $K\overline{K}$ threshold. $J \leq 1$ partial waves control $\pi\pi$ scattering in this region. Now each S and P-wave, $t(s)$ (dropping I, J labels for simplicity), has a zero at $s = s_0$. For the S-waves, these are demanded by the Adler condition; for the P-wave, the zero is kinematic being at threshold so $s_0 = 4\mu^2$. [1] The inverse, $f(s)$, of each of these partial wave amplitudes will thus have a simple pole at $s = s_0$, with residues r. Consequently we define

$$f_{pole}(s) \equiv \frac{r}{s - s_0}\,. \tag{2}$$

Now we shall assume that $\mid f(s) \mid < s$ as $s \to \infty$, so that each $f(s)$ satisfies a once subtracted dispersion relation with $s = s_1$, the subtraction point,

$$\begin{aligned} f(s) = f_{pole}(s) + c \quad &+ \quad \frac{(s-s_1)}{\pi} \int_{4\mu^2}^{\infty} \frac{ds'}{(s'-s_1)(s'-s)} \,\text{Im}\, f(s') \\ &+ \quad \frac{(s-s_1)}{\pi} \int_{-\infty}^{0} \frac{ds'}{(s'-s_1)(s'-s)} \,\text{Im}\, f(s') \quad . \end{aligned} \tag{3}$$

$\text{Im}\, f(s)$ is to be evaluated above both cuts; c is a constant simply related to the value of the inverse amplitude at the subtraction point $s = s_1$. Care must be taken if s_1 is chosen to be the position of the simple pole in Eq. (2), i.e. $s_1 = s_0$, then

$$c = \lim_{s \to s_0} \left(f(s) - f_{pole}(s) \right) \quad .$$

Since χPT is believed to describe $\pi\pi$ scattering in the subthreshold region quite accurately, the idea is to use its predictions to fix the position of the chiral pole ($s = s_0$) in the inverse amplitude and its residue r and the subtraction constant c, from the value of $f(s)$ at the subthreshold subtraction point. The partial wave may well converge faster than we assume Eq. (3), so that subtractions are not needed. However, the advantage of making a subtraction is that the more distant parts of the cut discontinuities play less of a role for the region of interest, $-0.5 < (s - 4\mu^2) < 0.5$ (GeV^2). The physics contained in these distant and poorly known contributions is replaced by the subthreshold subtraction term fixed by χPT.

[1] Higher partial waves have higher order zeros, of course.

To evaluate the dispersive representation of Eq. (3), we must know the imaginary parts; clearly

$$\mathrm{Im}\, f(s) = \mathrm{Im}\, \frac{1}{t(s)} = -\, \frac{\mathrm{Im}\, t(s)}{|\, t(s)\,|^{\,2}} \quad . \tag{4}$$

For $4\mu^2 < s \leq 1$ GeV^2, this just equals $-\rho$ in the elastic region, Eq. (1). The fact that the low energy right hand cut is specified by non-linear unitarity, Eq. (1), is a key step in building non-perturbative (and hence resonance) physics into the amplitudes $t(s)$. Indeed, since the elastic region extends essentially up to $K\overline{K}$ threshold, the right hand cut contribution of Eq. (3) can be reliably computed up to 750 MeV or so for the $I = 0$ S-wave and even higher for the $I = 2$ S-wave and $I = 1$ P-wave, for which the inelasticity is naturally weaker. We therefore set $\mathrm{Im}\, f(s) = -\rho(s)$ everywhere along the right hand cut as a reasonable approximation. The right hand cut integral of Eq. (3) can then be performed analytically and involves the Chew-Mandelstam function $\overline{J}(s)$ of one loop χPT [1], so that the integral is just $-16\pi(\overline{J}(s) - \overline{J}(s_1))$. However, the left hand cut is also crucial and we adopt a number of different schemes for its calculation, which we now describe.

Scheme I involves the simplest of all assumptions and sets the left hand cut discontinuity equal to zero. Of course, this violates crossing symmetry. It is impossible for the right hand cut to be non-zero and the left hand cut, generated by exchange forces, to be zero for amplitudes that are crossing symmetric as $\pi\pi$ is. Nevertheless, this provides a base from which to judge the dependence on the assumed left hand cut. The dispersive representation of Eq. (3) is evaluated with the subtraction constant specified by one loop χPT at $s_1 = 4\mu^2/3$ — a point conveniently between the two cuts. This we call scheme I.

Scheme II is to assume that the left hand cut discontinuity is given by one loop χPT out to $s = -(M^2 - 4\mu^2)$ with M typically 0.5-0.6 GeV and to assume it to be constant beyond that. This is in keeping with the notion that χPT predictions may be believed for $t, u \leq (0.6\ \mathrm{GeV})^2$ and that the distant left hand cut should not have too big an effect on the direct channel amplitude for $s < 1$ GeV^2. The subtraction term is fixed as in Scheme I with $s_1 = 4\mu^2/3$. As an illustration we plot in Fig. 1 the inverse $I = 0$ S-wave amplitude (as an example) in Scheme II. We see how the subthreshold

pole dominates the low energy amplitude throughout the region of $|s| < 1$ GeV^2. This spotlights the perils of neglecting its appearance [7]. In no sense can the residue of the pole be regarded as small [9]. In Fig. 2 we plot $f(s) - f_{pole}(s)$, again for the $I = 0$ S-wave, to indicate the difference using Scheme I or II makes to the physical region amplitude we wish to compare with experiment.

Scheme III is a stronger assumption, closer to that of Dobado and Peláez [7]. This is to note that one loop χPT satisfies unitarity (perturbatively) along the right hand cut, viz. Eq. (1), by

$$\mathrm{Im}\, t^{(1)}(s) \;=\; \rho \;\mid t^{(0)}(s) \mid^2, \tag{5}$$

where the bracketed superscripts label the order in the chiral expansion at which the whole partial wave is computed. It is then useful to note that the tree level amplitudes have the simple structure

$$t^{(0)} \;=\; \frac{s - s_0^{(0)}}{r^{(0)}} \tag{6}$$

where $s_0^{(0)}$ is the position of the zero (Adler zero for the S-waves, threshold zero for the P-wave) and $r^{(0)}$ is the residue of the corresponding pole in the inverse amplitude. As is well-known [3],

$$\begin{aligned} s_0^{(0)} &= \mu^2/2 \qquad \text{for the } I = 0 \;\; S-\text{wave}, \\ &= 4\mu^2 \qquad \text{for the } I = 1 \;\; P-\text{wave}, \\ &= 2\mu^2 \qquad \text{for the } I = 2 \;\; S-\text{wave}. \end{aligned} \tag{7}$$

with residues

$$\begin{aligned} r_0^{(0)} &= 16\pi\, F^2 \qquad \text{for the } I = 0 \;\; S-\text{wave}, \\ &= 96\pi\, F^2 \qquad \text{for the } I = 1 \;\; P-\text{wave}, \\ &= -32\pi\, F^2 \qquad \text{for the } I = 2 \;\; S-\text{wave}. \end{aligned} \tag{8}$$

where F is the pion decay constant in the chiral limit, $F = 0.94 F_\pi$ viz. [1]. In scheme III we assume along the left hand cut too that

$$\mathrm{Im}\, \frac{1}{t(s)} \;\equiv\; -\frac{\mathrm{Im} t(s)}{\mid t(s) \mid^2} \;\simeq\; -\frac{\mathrm{Im} t^{(1)}(s)}{(t^{(0)}(s))^2} \;. \tag{9}$$

This allows us to avoid explicitly evaluating a dispersive representation [8, 7], as follows : the one loop χPT amplitude $t^{(1)}$ grows asymptotically like s^2 modulo logarithms. Let us consider the function

$$\begin{aligned}\Delta t(s) \equiv t^{(1)}(s) &- t^{(1)}(s_1) - (s-s_1)\frac{d}{ds}t^{(1)}(s_1) \\ &- \frac{1}{2}(s-s_1)^2\frac{d^2}{ds^2}t^{(1)}(s_1)\end{aligned} \tag{10}$$

where s_1 is again a subtraction point in the subthreshold region. Then the function $\Delta t(s)/(s-s_1)^2$ will satisfy a once subtracted dispersion relation with zero subtraction constant, so that

$$\begin{aligned}\frac{\Delta t(s)}{(s-s_1)^2} &= \frac{(s-s_1)}{\pi}\int_{4\mu^2}^{\infty} ds' \frac{\mathrm{Im}\, t^{(1)}(s')}{(s'-s_1)^3(s'-s)} \\ &+ \frac{(s-s_1)}{\pi}\int_{-\infty}^{0} ds' \frac{\mathrm{Im}\, t^{(1)}(s')}{(s'-s_1)^3(s'-s)}\end{aligned} \tag{11}$$

This is just the statement that the amplitudes of χPT are analytic in the cut plane. Conveniently, choosing the subtraction point s_1 to be the position of the tree level zero, i.e. $s_1 = s_0^{(0)}$, we have noting Eq. (6)

$$\begin{aligned}\frac{\Delta t(s)}{(t^{(0)}(s))^2} &= \frac{\left(s-s_0^{(0)}\right)}{\pi}\int_{4\mu^2}^{\infty} ds' \frac{\mathrm{Im}\, t^{(1)}(s)}{\left(s'-s_0^{(0)}\right)(s'-s)(t^{(0)}(s'))^2} \\ &+ \frac{\left(s-s_0^{(0)}\right)}{\pi}\int_{-\infty}^{0} ds' \frac{\mathrm{Im}\, t^{(1)}(s)}{\left(s'-s_0^{(0)}\right)(s'-s)(t^{(0)}(s'))^2}\end{aligned} \tag{12}$$

Now using Eqs. (5,9), Eq. (3) and Eq. (12) can be simply added to give :

$$\begin{aligned}\frac{1}{t(s)} &= \frac{r}{s-s_0} + c - \frac{t^{(1)}(s)}{(t^{(0)}(s))^2} + \frac{t^{(1)}(s_0^{(0)})}{(t^{(0)}(s))^2} \\ &+ \frac{r_0}{t^{(0)}(s)}\frac{d}{ds}t^{(1)}(s_0^{(0)}) + \frac{1}{2}(r_0)^2\frac{d^2}{ds^2}t^{(1)}(s_0^{(0)})\end{aligned} \tag{13}$$

Uniquely for the P-wave, the zero of the full partial wave amplitude and that of the tree level approximation are at the same position, viz. $s_0^{(0)} = s_0 = 4\mu^2$. Then for the P-wave amplitude, we have

$$\frac{1}{t(s)} = \frac{1}{t^{(0)}(s)}\left(\frac{r}{r_0}+\frac{r_0}{r}\right) - \frac{t^{(1)}(s)}{(t^{(0)}(s))^2} - \frac{1}{2}(r^2-r_0^2)\frac{d^2}{ds^2}t^{(1)}(s_0^{(0)}) \quad (14)$$

If we further assume that the P-wave scattering length for the full χPT amplitude is the same as for the tree level approximation, then $r = r_0$ and we obtain [2]

$$\frac{1}{t(s)} = \frac{2}{t^{(0)}(s)} - \frac{t^{(1)}(s)}{(t^{(0)}(s))^2}$$

i.e.

$$t(s) = \frac{t^{(0)}(s)^2}{2t^{(0)}(s) - t^{(1)}(s)} \quad (15)$$

which is the $[1,1]$ Padé approximant introduced by Truong [8]. But note the key chain of assumptions needed to deduce this.

This brings us to **scheme IV**. This is again to assume the left hand cut discontinuity for all $s < 0$ is given by Eq. (9) and further to assume for each all orders partial wave amplitude that the position of the zero and the slope there are both just as for the tree level amplitude, i.e. $s_0 = s_0^{(0)}$ and $r = r_0$. This gives Eq. (15) for each S and P-wave amplitude. This is the scheme of Dobado and Peláez [7]. Of course, the S-wave zeros crucially move making this approximation poor, as we shall see.

Each of these schemes provides a continuation into the physical region of the predictions of χPT, that are assumed exact in the neighbourhood of the subtraction point in the subthreshold region. Though of course the underlying chiral amplitudes satisfy crossing symmetry exactly at each order, these continuations do not. We can test this failure by evaluating the five crossing sum rules that involve just the S and P-waves. If these relations were exactly satisfied they guarantee that there exists a $\pi\pi$ amplitude with the correct crossing properties with these precise $\ell = 0$ and 1 partial waves. In the appendix, we detail what these relations are and specify a measure by which we tell how well each of our approximations satisfies crossing. We tabulate the results in the next section.

[2] n.b. $t^{(1)}(s)$ means the full one loop partial wave and not just the one loop correction of Refs. [8, 7].

3. Results

In this section we display the results of the calculation of the 3 lowest partial wave amplitudes according to each of the four Schemes (described in the last section) for approximating the left hand cut contribution. To determine the subtraction term c and pole position s_0 and residue r of Eqs. (2,3) from χPT to one loop order, we have to choose values for the parameters $\overline{\ell}_i$ of the $SU(2)$ Chiral Lagrangian. As a guide we take the values [10]

$$\overline{\ell}_1 = -0.3, \;\; \overline{\ell}_2 = 4.5 \; . \tag{16}$$

The formulae for the $\pi\pi$ invariant amplitude to one loop are taken from Eq. (17.1) of Ref. [1], in which recall $F = 0.94 F_\pi$ where $F_\pi = 93$ MeV. The resulting elastic partial waves can then be expressed in terms of the corresponding phase-shift δ_J^I by way of the standard representation

$$t_J^I(s) \; = \; \frac{1}{\rho} \, \sin\delta_J^I \, \exp\left(i\delta_J^I\right) \qquad . \tag{17}$$

In Figs. 3-5, we show the phase-shifts for the $I = 0, 2$ S-waves and the $I = 1$ P-wave from each of the calculational schemes, together with experimental data from the LBL analysis of Protopopescu et al. [11], the CERN-Munich results of Ochs [12] and of Hoogland et al. [13], and the K_{e4} results of Rosselet et al. [14]. The curves I, II, III show rather dramatically how changing the left hand cut discontinuity, while keeping the same underlying chiral perturbative amplitude (i.e. the same subtraction constant c, pole position s_0 and residue r in Eqs. (2,3,13)), alters the partial waves in the physical region. Fig. 4 illustrates how the left hand cut (which is produced by exchange forces) determines the generation of the ρ-resonance — a fact on which the *bootstrap* principle was based [6]. Changing from curves III to IV illustrates the effect of assuming the chiral pole's position and residue are as in the tree level amplitude (without altering the left hand cut discontinuity), implicit in the Padé-like summation of Refs. [8, 7]. This demonstrates that a scheme like IV cannot be regarded as an accurate way of determining the Lagrangian parameters $\overline{\ell}_I$ $(i = 1, 2)$. In fact, we see that, with the choice of the $\overline{\ell}_i$ of Eq. (16), Scheme II provides the best agreement with data. However, by a suitably different choice of the Lagrangian parameters any of the

other Schemes can be made to agree better with experiment — but not for all of the waves at one time as we now explain.

An independent way to test the consistency of each approximation scheme is to check how well crossing symmetry is fulfilled by the resulting 3 lowest partial waves. The problem of how to express the consequences of crossing symmetry — a property of the full amplitude — in terms of a finite number of partial waves was solved more than 25 years ago by Balachandran and Nuyts [15] by considering the amplitudes in the Mandelstam triangle. An explicit realisation of these subthreshold relations, known as *crossing sum rules*, was given shortly thereafter by Roskies [16]. These provide a necessary and sufficient set of conditions for crossing. In the Appendix we give the five sum rules that involve just the S and P-waves.

Scheme	l.h.cut	cross1	cross2	cross3	cross4	cross5
I	none	1.0	0.6	0.5	0.9	0.6
II	Eq. (3)	0.2	0.1	0.1	0.2	0.0
III	Eq. (13)	1.0	0.2	1.1	1.3	0.9
IV	Eq. (15)	1.3	0.0	1.5	1.5	1.2

Table 1: Tests of the crossing sum rules, Eqs. (A1-5), as defined by the ratio R in Eq. (A6) each expressed as a percentage.

In Table I we show how the partial waves calculated in each scheme fulfil these relations in terms of the measure defined in Eq. (A6). We see that if the partial waves have no left hand cut (Scheme I) crossing is violated by 0.5-1.0%. In contrast, if the nearby part of the left and right hand cuts are given by one loop χPT (Scheme II), then the violation is only 0.1-0.2%. Since having no left hand cut, but explicitly having a right hand cut, is clearly in violation of crossing symmetry, the 1% violation of Scheme I sets the scale for the level of violation. As already mentioned, by making the underlying chiral amplitude different by a different choice of the $\overline{\ell}_i$ a partial wave in any scheme can be brought into agreement with experiment. However, only for Scheme II with its

near crossing symmetry can this be achieved for each partial wave simultaneously. We see that Schemes III and IV, in which the left hand cut for the inverse amplitude is approximated by Eq. (9), give a larger violation than even having no left hand cut.

4. Conclusions

Dispersion relations for the inverse partial wave amplitudes provide a method of imposing a right hand cut structure consistent with unitarity. Thus this method is a useful way of continuing the predictions of χPT at any order, into the physical regions where the non-linearity of unitarity determines resonant behaviour. Considering $\pi\pi$ scattering, we have shown here how strongly these continuations depend on the assumed left hand cut discontinuity and on our knowledge of the position and residue of the subthreshold poles that are the key embodiment of chiral dynamics. We have shown how crossing symmetry allows us to select between different approximation schemes. Not surprisingly neglecting the left hand cut (and by inference exchange forces) violates crossing. However we have seen that the favoured Padé-like sums violate crossing even more strongly. Consequently, calculations based on such approximation schemes cannot be regarded as reliable ways of determining the Chiral Lagrangian parameters $\overline{\ell}_1$, $\overline{\ell}_2$.

The inverse amplitude method is a way of unitarising the predictions of χPT. However, different assumptions on how to implement the method have a considerable effect on the physical region predictions and the subsequent comparison with data. Reassuringly, the requirement of crossing symmetry brings closer agreement with experiment as our Scheme II demonstrates. This suggests a more reliable continuation of χPT into the physical region could be obtained by using the crossing sum rules to restrain the form of the left hand cut discontinuity and the corresponding values of the Lagrangian parameters $\overline{\ell}_1$, $\overline{\ell}_2$. Then the inverse amplitude method might achieve the precision phenomenology earlier treatments claim and be able to predict the resonance poles that control low energy meson scattering processes.

Acknowledgements

One of us (MRP) is grateful to Dominique Toublan, Res Urech, Fernando Cornet and Jorge Portolés for initial discussions about the Inverse Amplitude Method. This would not have been possible without (i) the organisation of the "Workshop on the Standard Model at Low Energies" by Hans Bijnens and Ulf Meissner that took place at ECT* in Trento in May 1996 and (ii) the support of the EURODAΦNE Network that provided funds to attend this meeting under grant ERBCMRXCT920026 of the EC Human and Capital Mobility programme. To both ECT* and the EU thanks are due. The other author (MB) is grateful to M. Anselmino, E. Predazzi and R. Garfagnini for permitting her to study at the University of Durham and to INFN (Sezione di Torino) for the necessary travel support.

Appendix A

Below we give the integral relations crossing symmetry imposes on the $\pi\pi$ partial wave amplitudes, $t_J^I(s)$, with isospin I and spin $J \leq 1$ [16] :

$$\int_0^{4\mu^2} ds\,(4\mu^2 - s)\,(3s - 4\mu^2)\,\Big(t_0^0(s) + 2t_0^2(s)\Big) = 0 \tag{A1}$$

$$\int_0^{4\mu^2} ds\,(4\mu^2 - s)\,\Big(2\,t_0^0(s) - 5t_0^2(s)\Big) = 0 \tag{A2}$$

$$\int_0^{4\mu^2} ds\,(4\mu^2 - s)\,(3s - 4\mu^2)\,\Big(2\,t_0^0(s) - 5t_0^2(s)\Big) + 9\int_0^{4\mu^2} ds\,(4\mu^2 - s)^2\,t_1^1(s) = 0 \tag{A3}$$

$$\int_0^{4\mu^2} ds\,(4\mu^2 - s)\,s^2\,\Big(2\,t_0^0(s) - 5t_0^2(s)\Big) + 3\int_0^{4\mu^2} ds\,(4\mu^2 - s)^3\,t_1^1(s) = 0 \tag{A4}$$

$$\int_0^{4\mu^2} ds\,(4\mu^2 - s)^2\,s^2\,\Big(2\,t_0^0(s) - 5t_0^2(s)\Big) + 3\int_0^{4\mu^2} ds\,(4\mu^2 - s)^2\,(8\mu^2 - 3s)\,s\,t_1^1(s) = 0 \quad . \tag{A5}$$

Each of these relations can be written generically as

$$\int_0^{4\mu^2} ds\,\omega(s)\,\sum_I \alpha_I\;t_J^I(s) \;=\; 0 \quad .$$

where the α_I are constants. A measure of how close any integral is to zero can be assessed by forming the ratio

$$R \;=\; \frac{\int_0^{4\mu^2} ds\,\omega(s)\;\sum_I \alpha_I\;t_J^I(s)}{\int_0^{4\mu^2} ds\,\omega(s)\;\mid \sum_I \alpha_I\;t_J^I(s)\mid} \tag{A6}$$

This is the quantity expressed as a percentage that we quote in Table I for each of the five sum rules of Eqs. (A1-5). As is well known the tree level amplitudes [3] satisfy crossing exactly, we could have defined an alternative measure by replacing each partial wave $t_J^I(s)$ by its difference from the tree level approximation. This gives values for the corresponding ratio R a factor of two larger for all the numbers in Table I, leaving the qualitative comparison the same.

References

[1] J. Gasser and H. Leutwyler, Ann. Phys. (NY) bf 158 (1984) 142.

[2] J.F. Donoghue, E. Golowich and B.R. Holstein, "Dynamics of the Standard Model", pub. Cambridge 1994.

[3] S. Weinberg, Phys. Rev. Lett. **17** (1966) 616.

[4] "Chiral Dynamics: Theory and Experiment", Proceedings of the MIT Workshop, July 1994 (ed. A.M. Bernstein and B.R. Holstein) pub. Springer-Verlag 1995.

[5] Mini-proceedings of Workshop on the Standard Model at Low Energies, ECT* , Trento, May 1996 (ed. J. Bijnens and U.-G. Meissner) hep-ph 9606301.

[6] R. J. Eden, "High Energy Collisions of Elementary Particles", pub. Cambridge 1967.

[7] A. Dobado and J.R. Peláez, LBL-38645, UCM-FT 3/96 (April, 1996) hep-ph 9604416, Z.Phys. **C57** (1993) 501.

[8] T.N. Truong, Phys. Rev. Lett. **61** (1988) 2526, ibid. **67** (1991) 2260.

[9] A. Dobado and J.R. Peláez, Phys. Rev. **D47** (1992) 4883, Z.Phys. **C57** (1993) 501.

[10] M.R. Pennington and J. Portolés, Phys. Lett. **B344** (1995) 399.

[11] S.D. Protopopescu et al., Phys. Rev. **D7** (1973) 1279.

[12] W. Ochs, Univ. of Munich thesis (1973);
B. Hyams et al., Nucl. Phys. **B64** (1973) 134.

[13] W. Hoogland et al., Nucl. Phys. **B126** (1977) 109.

[14] L. Rosselet et al., Phys. Rev. **D15** (1977) 574.

[15] A.P. Balachandran and J. Nuyts, Phys. Rev. **172** (1968) 1821.

[16] R. Roskies, Nuovo Cimento **65A** (1970) 467;
C.S. Cooper and M.R. Pennington, J. Math. Phys. **12** (1971) 1509.

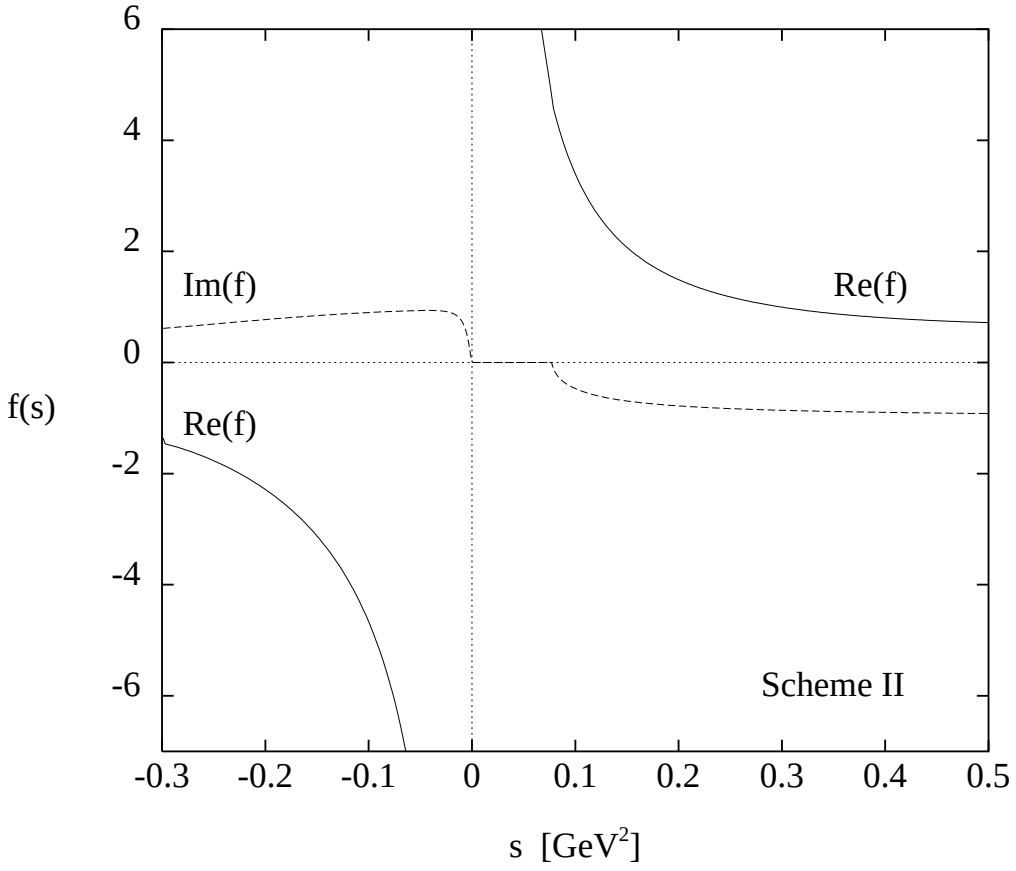

Figure 1: Real and imaginary parts of the $\pi\pi$ $I = 0$ S-wave inverse amplitude, $f(s) = 1/t_0^0(s)$ for $s+i\epsilon$, from Eq. (3), calculated using Scheme II. Note the way the pole, which is the Adler zero in the partial wave, dominates the behaviour of the inverse.

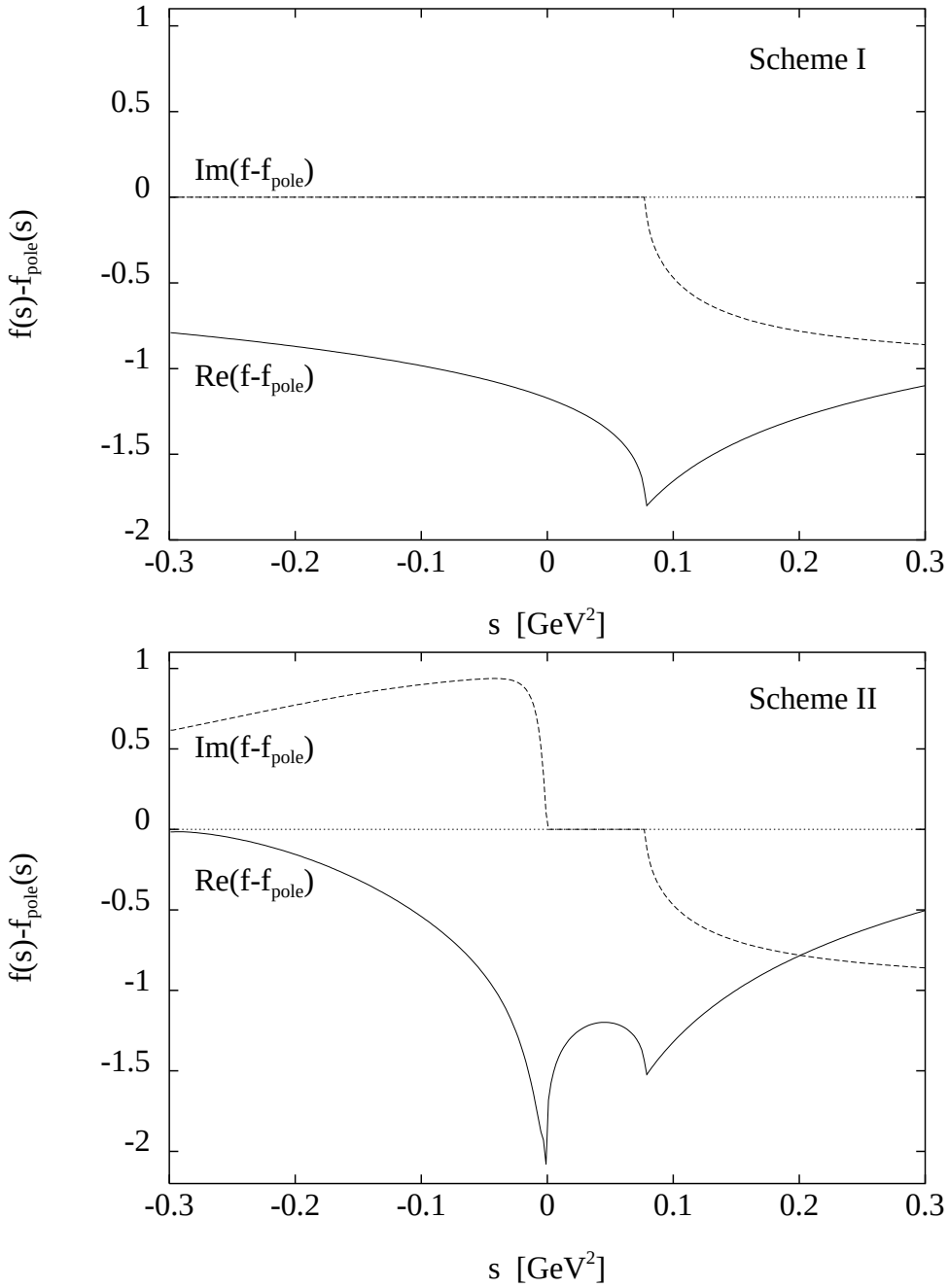

Figure 2: Real and imaginary parts of the $\pi\pi$ $I = 0$ S-wave inverse amplitude without the contribution of the pole, $f(s) - f_{pole}(s)$, for $s + i\epsilon$, calculated from Eq. (3) according to Scheme I, which has no left hand cut, and Scheme II. Notice how the behaviour of the real part (solid line) of the amplitude at $s = 0$ and $s = 4\mu^2$ reflects the strength of the relevant cut discontinuity, which is just the imaginary part (dashed line).

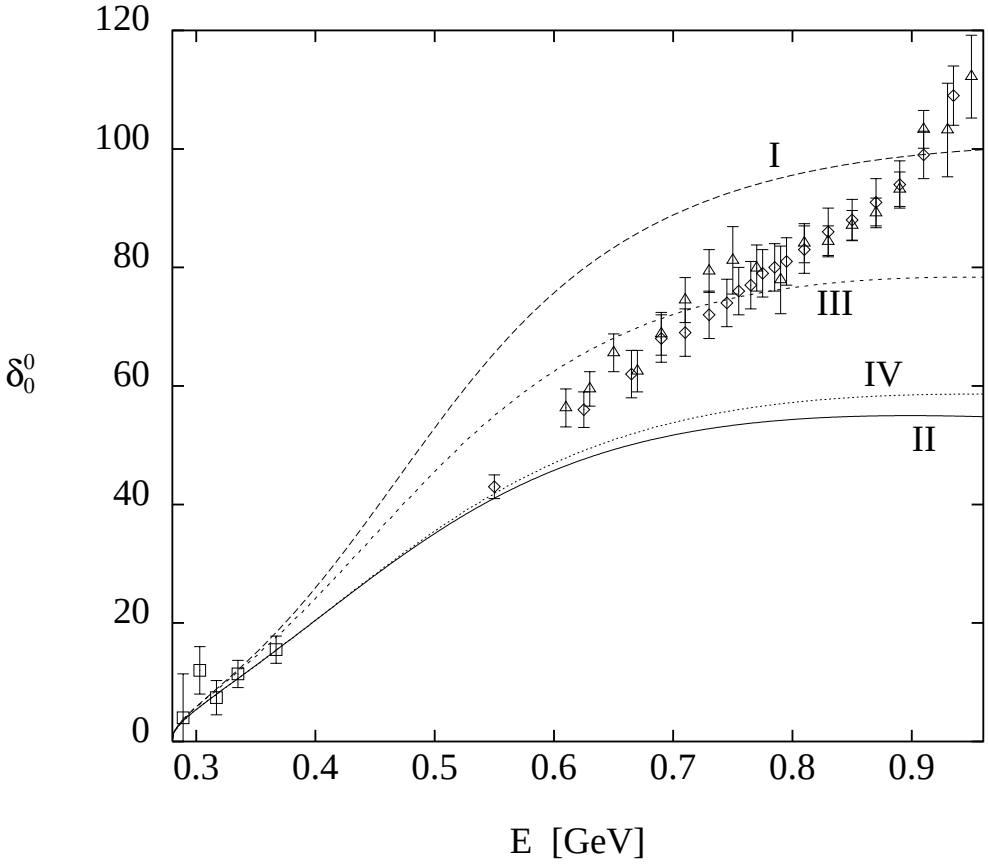

Figure 3: The $\pi\pi$ $I = 0$ S-wave phase shift, δ_0^0 in degrees, below $K\overline{K}$ threshold as a function of $\pi\pi$ mass $E = \sqrt{s}$. The dashed line is the result obtained with no left hand cut contribution (Scheme I); the solid line comes from the explicit evaluation of the left hand cut dispersive integral (Scheme II); the dotted lines are obtained with additional summation assumptions (Schemes III and IV). The experimental results are from Protopopescu et al. [10] (diamonds), the energy-independent analysis by Ochs [11] (triangles) and the K_{e4} decay data of Rosselet et al. [13] (squares).

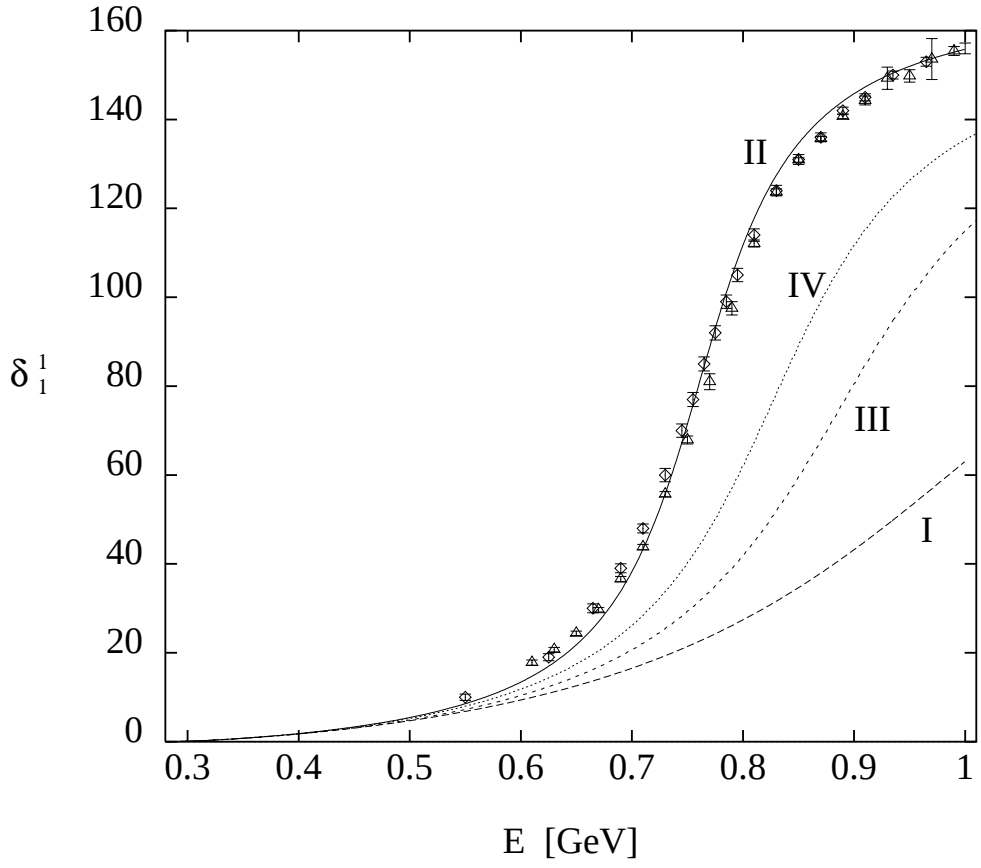

Figure 4: The $\pi\pi$ $I = 1$ P-wave phase shift, δ_1^1 in degrees, below $K\overline{K}$ threshold as a function of $\pi\pi$ mass $E = \sqrt{s}$. The dashed line is the result obtained with no left hand cut contribution (Scheme I); the solid line comes from the explicit evaluation of the left hand cut dispersive integral (Scheme II); the dotted lines are obtained with additional summation assumptions (Schemes III and IV). The experimental data are from Protopopescu et al. [10] (diamonds) and the energy-independent analysis by Ochs [11] (triangles).

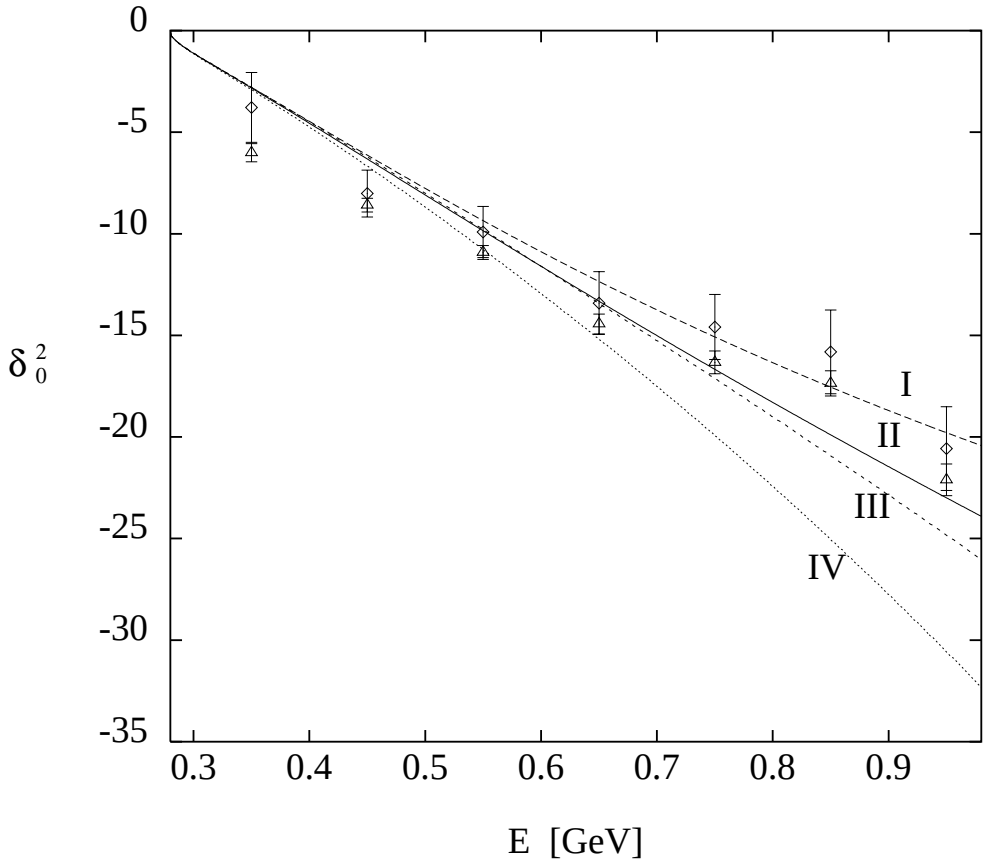

Figure 5: The $\pi\pi$ $I = 2$ S-wave phase shift, δ_2^2 in degrees, below $K\overline{K}$ threshold as a function of $\pi\pi$ mass $E = \sqrt{s}$. The dashed line is the result obtained with no left hand cut contribution (Scheme I); the solid line comes from the explicit evaluation of the left hand cut dispersive integral (Scheme II); the dotted lines are obtained with additional summation assumptions (Schemes III and IV). The experimental data are from the analyses by Hoogland et al. [12].